

# PROJECT DESCRIPTION

## Results of Prior NSF Support

**AWARD:** NSF Division of Atmospheric Sciences Grant DAS-0222171, 7/02 - 9/06; Collaboration in Mathematical Geosciences (CMG): *Microstructural Controls on Transport Processes in Geophysical Systems*. PI: K. M. Golden, U. of Utah (UU), co-PI: H. Eicken, U. of Alaska, Fairbanks (UAF), \$733,000, including a Research Experiences for Undergraduates (REU) Supplement to UU (\$63,000).

**SUMMARY OF RESULTS:** The vertical fluid permeability  $k$  of sea ice constrains a broad range of processes, such as the growth and decay of seasonal ice, the evolution of summer ice albedo, and biomass build-up. However, studies of  $k$  and its dependence on brine porosity  $\phi$  and microstructure were sparse. We developed a unified theory for  $k(\phi)$  which closely captures lab and field data [70, 72, 148]. Our analytical and numerical modeling is based on rigorous bounds [72], lattice and continuum percolation theory [67, 58, 70], hierarchical models [70], and random pipe networks [148]. We found that sea ice displays universal transport properties remarkably similar to crustal rocks. X-ray computed tomography and pore structure analysis provided an unprecedented look at the brine phase and its connectivity [70]. These advances have also allowed us to predict anisotropic percolation thresholds in sea ice, and to compute, for the first time in natural materials, various connectedness functions of classical lattice percolation theory [112]. In related work, we obtained bounds on the complex permittivity of sea ice at 50 MHz, and inverted the data to get bounds on brine porosity [75]. Finally, we used percolation models to help explain anomalies in resistivity data from rocks deep in the mid-crust of the Southern Alps of New Zealand [139].

Our work on permeability has had broad impact. From 2007 through mid-2009, Golden has been invited to give 32 lectures on this work at universities and major conferences in the US and abroad. This work has also received extensive media coverage, including *Geotimes*, *Ars Technica*, *Electrical Engineering Times*, and a two page profile of Golden and his work at the interface of mathematics and climate change in *Science* (scheduled for 27 March 2009), radio, television and web interviews, and numerous invited lectures to general audiences and student groups. For example, Golden was invited by the AMS to give a Congressional Luncheon Briefing on Capitol Hill in Washington D. C. in November 2007.

**CONTRIBUTION TO HUMAN RESOURCES:** This award has provided partial support for three graduate students, Jeremy Miner and Lars Backstrom at UAF, and Ben Murphy at UU, a post-doc, Daniel Pringle at UAF, two technician/programmers, and six UU undergraduates from a range of majors. Support included travel for collaborative work between UU and UAF, and Arctic field experience for five of the undergraduates. All students were involved in publications and giving lectures. For example, Amy Heaton [70, 72] began with Golden in his freshman Calculus class, and has given presentations at an Undergraduate Math Res. Conf. at Ohio State (2003), the Physics Dept. at Victoria University, NZ (2004), the Utah State Legislature (2004), and with Golden in the US Congress in June 2003. Four of the undergraduates are in top Ph.D. programs in math or science, one completed a Masters in EE at Columbia, and one completed an M.D. at UU. In 2007 Kellen Petersen won the Research Scholar Award, the highest undergraduate research honor in the College of Science at UU. In 2008 Adam Gully won the same award.

**AWARD:** NSF Division of Mathematical Sciences Grant DMS-0537015, 9/1/05 - 8/31/09, UU, *Analysis and Computation of Electromagnetic Transport in Composite Materials*. PI: K. M. Golden, co-PI: D. Dobson, \$403,000; including an REU Supplement (\$61,000).

**SUMMARY OF RESULTS:** We have been investigating novel approaches to some challenging issues in electromagnetic transport in composites. Several results have been obtained in the effort to extend the analytic continuation method for bounding the effective complex permittivity beyond quasistatics to dynamics [123, 122]. We've obtained rigorous and numerical results on a new effective complex permittivity defined for finite frequency, and how it behaves in certain limits. Related work on structural optimization for diffraction has been submitted [42].

Electrorheological (ER) fluids are particle suspensions that exhibit a rapid fluid/solid transition when an applied electric field exceeds a critical value. Particles can form columns or fractal networks similar to diffusion limited aggregation (DLA). Our work on statistical mechanics of ER fluids has focused on characterizing the ground states as minimizers of a new logarithmic "free energy" (joint with Ping Sheng of HKUST). We are also studying high-contrast limits of the free energy and spectral problems for the Laplacian, and related

simulations of DLA. We have derived the effective permittivity of composites using statistical mechanics, and found a deep connection with the theory of random matrices and ensembles of orthogonal polynomials [88, 40, 105]. We have conducted experiments on ER fluids, imaging their microstructural evolution with high speed cameras, and measuring shear viscosity in parallel plate and circular geometries.

An interesting composite where many key issues of EM transport arise is sea ice – which shares connectivity threshold behavior with ER fluids. In Sept.-Oct. 2007, Golden and math student Adam Gully participated in the Sea Ice Physics and Ecosystem eXperiment (SIPEX) in Antarctica aboard the Australian icebreaker *Aurora Australis*, as part of the International Polar Year (IPY) activities. We used an earth resistance tester in a Wenner array to obtain DC resistivity profiles of the ice, and adapted the set-up to measure the vertical conductivity of cores [71]. We also made the first measurements of permeability in Antarctic pack ice, and conducted tracer experiments on ice blocks. We used a wave generator and oscilloscope to measure the complex permittivity of a sea ice core from 10 KHz to 15 MHz, using the four probe array.

The sea ice work, particularly Golden and Gully's participation in the SIPEX expedition, is having broad impact. The AMS has featured Golden's Antarctic work in a "Mathematical Moment" for the general public on its website, including an extensive interview, and Golden was interviewed by satellite phone for Public Radio during the expedition. Golden has produced a DVD giving an overview of the science on SIPEX, and the excitement and beauty of venturing to Antarctica. This footage has been shown on TV and to many student, scientific, and general audiences, including the US Congress and the largest visual arts college in the US, Columbia College Chicago (see [www.math.utah.edu/golden/media.html](http://www.math.utah.edu/golden/media.html) for details).

**CONTRIBUTION TO HUMAN RESOURCES:** Partial support for 5 math grad students Lyubima Simeonova, Ben Murphy, Russell Richins, Hwan Yong Lee, and Adam Gully, and 6 undergrads, Olakunle Eso, Megan Morris, Peter Sommerkorn, Dave Arcilesi, Kellen Petersen, and Christian Sampson. Simeonova will finish her Ph.D. in spring 2009, and Murphy is expected to finish his Ph.D. in spring 2010.

**AWARD:** NSF Office of Polar Programs, Arctic Sciences Grant ARC-0620124, Feb. 1, 2008 - Jan. 31, 2009, *Geoelectric Array Measurements of Sea Ice Porosity for Scientific and Operational in-situ Ice Property Assessments*. PI: H. Eicken, co-I: D. Pringle, UAF, \$31,627.

**SUMMARY OF RESULTS:** The aims of this project were to develop and field-test methods for making automated *in situ* DC resistivity measurements in sea ice. This enables tracking of the evolution of sea ice profile properties and fills a current gap in the real-time monitoring of local ice conditions needed to assess ice strength and trafficability. Surface resistivity soundings and cross-borehole DC resistivity tomography have been performed in land-fast sea ice at Barrow, Alaska. Following successful proof-of-concept measurements between two boreholes showing electrical anisotropy and thermal evolution through the melt season [111, 84], semi-automated measurements in four boreholes with lab measurements elucidated the dependence of the complex permittivity on pore microstructure. The combination of these lab and field efforts allowed us to obtain *in situ* measures of pore microstructure and its evolution [109].

**CONTRIBUTION TO HUMAN RESOURCES:** This project has fostered international interdisciplinary collaboration with a solid-earth geophysicist – collaborator on the present proposal, M. Ingham. Other synergistic benefits include instruction by Ingham, and attendance of a physics graduate student from New Zealand at an International Sea Ice Field Course in Barrow, Alaska, May 2008, organized by Eicken with more than 30 students participating and centering on the critical role of sea ice transport properties in the climate system. A chapter by Pringle and Ingham on ice transport properties for a handbook resulting from this course is in preparation [110].

**AWARD:** NSF Division of Mathematical Sciences Grant DMS-0508901, 07/01/05 - 06/31/08, *Inverse Homogenization for Microstructured Media*, PI: E. Cherkaev, \$79,887.

**SUMMARY OF RESULTS:** The inverse homogenization problem [32, 27] concerns recovery of microstructural information from measurements of effective properties of composites. The approach is based on reconstruction of the spectral measure  $\mu$  [27] in the Stieltjes representation of the effective tensor for two-component composites, developed in [10, 97, 61]. The problem of recovering  $\mu$  from effective measurements in an interval of frequency has a unique solution [27], however it is ill-posed. The reconstructed spectral density couples various effective properties of the same composite [27, 28, 34]. Having reconstructed it from the effective complex permittivity, one can compute other effective properties of the same

composite material. Efficient computational methods based on stabilization techniques have been developed for the reconstruction problem [29, 146, 33]. In [147] Padé approximation gave an elegant method for identifying the air bubble volume fraction from temperature or frequency dependent permittivity measurements. Wave propagation in nonlinear bistable materials was studied in [26], and finding optimal composite microstructures was reduced in [30, 31] to a minimax optimal design problem. Other work included extension of inverse homogenization methods to viscoelastic composites [104]. A novel method for identifying bone structure from measurements of the complex viscoelastic modulus was developed [17, 18, 19, 16, 20].

**CONTRIBUTION TO HUMAN RESOURCES:** Funds from this award were used to support two Ph.D. students, one of them graduated with the Ph.D. degree (fall 2007) and went on to a postdoctoral position, the other one is going to graduate in 2009.

**AWARD:** NSF Div. Math. Sci. Grant DMS-0602219, 5/17/2006 – 7/31/2011, UU, *EMSW21-VIGRE: Vertical Integration in Mathematics at the University of Utah*. PI: A. Bertram, coPI: D. Dobson, Senior Personnel: F. Adler, E. Cherkaev, K. M. Golden, N. Korevaar, G. Savin, K. Schmitt, P. Trapa, and J. Zhu, \$3,500,000. The UU Math. Dept. received two consecutive VIGRE awards in 2001 and 2006, supporting pre-college, undergraduate, graduate, and postdoctoral programs. As Director of Undergrad. Studies (2002-8), and as REU Coordinator (2003-7), Golden was responsible for the undergrad. components. Since 2001, they have so far supported 156 undergrads in REU programs, 58 grad students, and 17 postdocs. Golden led efforts to broaden our degrees, introducing new majors in Applied Math and in Statistics designed to promote double majoring and interdisciplinary studies. Rapid growth in the number of math majors has occurred.

**NSF AWARDS to Cynthia Furse:** NSF ECS-0080559 Design of Imbedded Microstrip Antennas for Wireless Communication and Remote Sensing; NSF ECS-0115157 Smart Wiring for In Situ Testing of Aging Wiring; NSF 0343282 Integrated Project-Based Design Curriculum ECE Department Level Curriculum Reform; NSF ECS-0330465 Sensors for Critical Fault Location for Aging Wire Networks; NSF ECS-0524720 Near-optimal Antenna Topology and Detection Strategy for Multiple-Input Multiple-Output (MIMO) Communication Systems; NSF 0652982 STEP – Utah’s Engineers: A Statewide Initiative for Growth 09/01/07 – 08/31/12, PI: Cynthia Furse, UU, \$2,000,000. This college-wide project seeks to increase the number of engineering graduates at UU through HS outreach, focusing on development of online and hands-on teaching modules for HS math, physics, and chemistry classes, and freshman/sophomore retention, through enhanced relationships with local high schools, and engineering career counseling. Participants include 7 engineering departments, Dept. of Educ., Dept. of Comm., State Board of Ed., etc. A sampling of results from the above awards are contained in the following publications: [46, 52, 53, 54, 80, 89, 93, 120, 124, 125].

## 1. Introduction

A confluence of recent theoretical, experimental, and technical advances has made it possible for us to propose a path toward *in situ*, electromagnetic monitoring of the internal microstructural state of sea ice, and key transport processes which it controls. These fluid and thermal processes mediate air-ice-ocean interactions, and are critical to the role that sea ice plays in the climate system and in hosting highly productive microbial communities. Transitions in transport properties effectively determine whether fluid fluxes through the ice can impact large scale heat and mass balances, or if nutrient supplies for algae and bacteria can be replenished. Such phenomena are important in the seasonal ice pack of Antarctica, where flooding of the surface and subsequent production of snow-ice is pervasive [67]. In a changing climate, the future trajectory of the Arctic ice pack may also depend critically on this process [107]. Sea ice albedo, a key agent in the dramatic decline of the summer Arctic ice pack, also depends on fluid flow [45]. Development of the proposed techniques to monitor and investigate fluid and thermal transport will require mathematical advances at the interface of homogenization for composites, percolation theory, spectral theory of partial differential equations, multiscale numerical modeling, random matrices, as well as inverse methods.

Sea ice exhibits an important transition in its fluid transport properties around a critical value of the brine volume fraction or porosity  $\phi$ . For  $\phi$  below  $\phi_c \approx 5\%$ , columnar sea ice is effectively impermeable to fluid flow, while for  $\phi$  above  $\phi_c$ , the ice is permeable. For a typical bulk salinity of 5 parts per thousand (ppt), this critical porosity  $\phi_c \approx 5\%$  corresponds to a critical temperature of  $T_c \approx -5^\circ\text{C}$ , known as the *rule of fives*. It was conjectured [67] that this behavior was due to a *percolation threshold*, or transition in the connectedness of the brine phase. A continuum percolation model for compressed powders used in

*stealthy* or radar absorbing coatings was adapted to predict  $\phi_c \approx 5\%$ , which explained Antarctic data on snow-ice growth and algal production.

The first recent development which will facilitate the advances we propose here is X-ray computed tomography (CT) of sea ice microstructure, and subsequent mapping of the binary images of ice and brine onto random graphs containing pore and throat size data [70, 112, 113, 56, 114]. In fact, analysis of these graphs provided the first direct evidence [70] of the connectivity transition conjectured in [67]. A sampling of our results is shown in Figure 1 [70, 112]. This mathematical characterization of the brine phase and its thermal evolution provides a critical step towards forward computations of transport properties and reconstructions of the microstructural state.

Another significant development has been Cherkaev's recent work on reconstructing the spectral measure  $\mu$  of the composite microgeometry from data on the effective complex permittivity tensor  $\epsilon^*$  [27, 29, 146, 147]. The measure  $\mu$  [61] is the spectral or eigenvalue density of a self-adjoint operator involving the indicator function taking the value 1 in brine and 0 in ice, and it encapsulates the link between microgeometry and transport. Through mathematical and computational analysis we'll be able to obtain detailed microstructural information from  $\mu$ , as well as other transport properties such as thermal conductivity or electrical resistivity [34]. Using spectral measures to obtain coefficients of fluid transport or advection-enhanced thermal transport will depend on the development of new representations, as well as our recent theoretical results on fluid permeability [70, 72, 148].

The problem of recovering  $\mu$  has a unique solution if  $\epsilon^*$  is known along an arc in the  $s$ -plane [27], where  $s = 1/(1 - h)$  and  $h = \epsilon_1/\epsilon_2$  with  $\epsilon_1$  the complex permittivity of brine and  $\epsilon_2$  the complex permittivity of ice. Since  $\epsilon_1$  depends on frequency  $\omega$  [127], an arc in the  $s$ -plane can be traced out as  $\omega$  is varied. Recovery of  $\mu$  thus requires measurements of  $\epsilon^*$  over a range of frequencies – a focus of our experimental efforts. Along with direct measurements on cores will be parallel efforts at modeling  $\epsilon^*(\omega)$ , the DC conductivity tensor, and their dependence on microstructure. We are particularly interested in the EM signature of sea ice near the percolation transition, to understand how to monitor this key phenomenon controlling so many processes important in studying climate.

Finally, the recent emergence of cross-borehole technology [111, 84] to image the electrical properties of sea ice in a three dimensional volume provides a key stepping stone toward monitoring the internal structure and transport characteristics of sea ice. Current versions can monitor the resistivity structure in the volume enclosed by the boreholes. When coupled with the efforts above, this method will be able to provide detailed knowledge of the internal state of sea ice. However, we will also be working to extend this technique to image the complex permittivity structure in the enclosed volume. Such an advance would close the circle, connecting the direct core measurements, forward modeling efforts, and microstructural reconstructions. Eventually, arrays of these EM monitors could be left in ice floes, transmitting their data to a satellite.

## 2. Sea Ice Microstructure and Transport Processes it Controls

**Geometry and Connectedness of the Brine Phase.** Columnar ice, which accounts for the bulk of the volume of Arctic sea ice and between 25% and 50% of Antarctic sea ice [141, 44, 135], grows through freezing of seawater onto the base of the ice sheet. Brine inclusions in columnar ice typically occur in vertically oriented, subparallel sheets or layers of brine separated by ice lamellae. As an ice horizon that accretes at the base of the ice cover ages and cools with further growth beneath, the brine inclusions shrink in size. Eventually, further freezing pinches the brine layers and pores segregate into partially connected arrays. The classic pore microstructural model of Assur [3] suggests that this pore space segregation occurs in two steps, with formation of cylindrical tubes that eventually separate into strings of ellipsoidal inclusions. Recent work [90, 15], in particular X-ray microtomography data reported in [70] (see also Fig. 1), indicate that pore space thermal evolution is more complicated, with a high degree of convolution in pore space morphology. However, more detailed analysis [112] also indicates that pore space connectivity evolves via a non-linear transition with critical behavior of transport described by percolation theory [70, 67]. Experimental errors in fluid measurements alone limit assessment of the applicability of percolation theory and theories of critical behavior of transport. However, our recent microstructural studies and preliminary work on sea ice dielectric and DC conductivity properties [75, 71] suggest transitional behavior in EM properties. Combining different approaches holds great promise in further understanding the transport behavior of sea ice as a composite medium, which motivates the work proposed here.

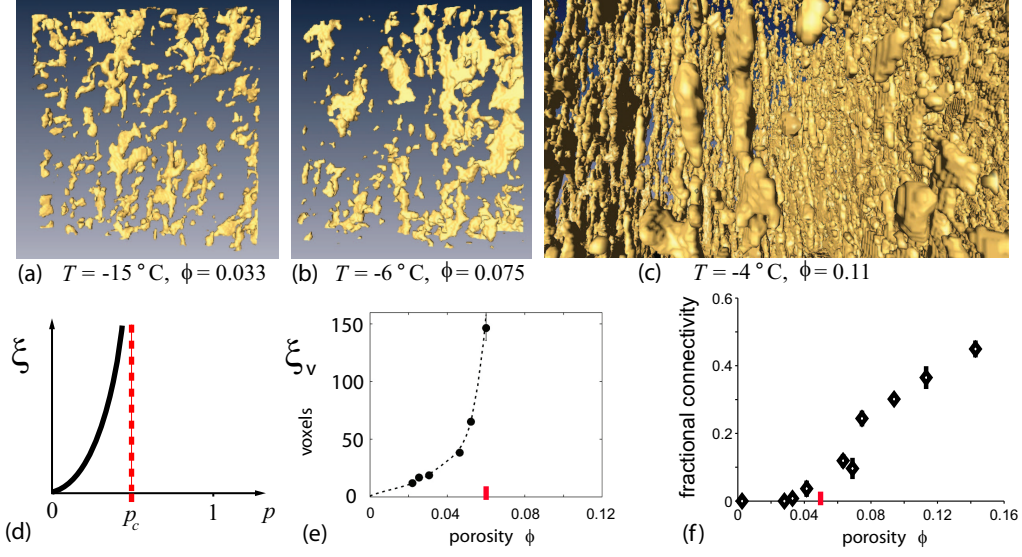


Figure 1: (a-c) X-ray CT volume renderings of the brine phase within a lab-grown sea-ice single crystal with  $S = 9.3$  ppt. The (non-collocated)  $8 \times 8 \times 2$  mm sub-volumes in (a) and (b) illustrate changes in brine connectivity during warming, with no top to bottom connections in (a) and one in (b). An image from a cylinder of height 8 mm and diameter 21 mm with many such connections is shown in (c). A graph of the divergence of the correlation length at the percolation threshold is shown for a lattice model in (d), and for brine in the vertical direction in sea ice in (e), with data from mapping the tomographic images onto random graphs [112]. (f) Fractional connectivity is the proportion of inclusions connecting the upper surface to the lower surface. The bulk threshold should slightly exceed the smaller-scale threshold of about 0.04 here.

**Mapping the Brine Microstructure onto Networks.** Realistic network models of the brine phase can be derived from porous media analysis of 3-D micro-tomography images. Approaches include the well-established 3DMA package (3-Dimensional Medial Axis, e.g [91, 92, 114] and the developmental Tight Dual Model (TDM) [56, 55]. We have worked closely with developers of both packages [112, 113, 70]. In both cases, a 3-D graph of nodes and edges is derived from the pores and throats. In general terms, the steps are: (1) represent the pore space by a polyhedral complex; (2) decompose this digital pore space into pores and throats, and compute individual characteristic radii; (3) map these to nodes and edges, tagged with their respective radii. To link tomography and network models [148, 70], and to provide the forward basis for accurate inversions, we will couple these approaches by computing transport in these experimentally derived pore-throat networks.

**Columnar vs. Granular Ice.** To date, columnar microstructures have received disproportionate attention, mostly due to their prevalence in Arctic sea ice and their importance in undisturbed ice growth [141, 90, 140]. Granular ice, however, is predominant in the Antarctic [85, 145, 44] and exhibits substantially different pore microstructure, with a near-complete lack of intragranular inclusions and a film of brine enveloping individual grains. Here, we propose a comparison between columnar ice (mostly existing data, such as in [70, 112]) and new granular ice data, from natural and laboratory grown samples. Such an approach is particularly relevant for remote sensing, since the penetration depth of microwaves typically extends only into the surface granular ice layers prevailing both in the Arctic and Antarctic. Moreover, we expect differences in transitional behavior in columnar vs. granular ice, such as in the value of  $\phi_c$ . The Antarctic field experiments will afford opportunities to measure electrical and fluid transport in granular ice.

**Transport Processes in Sea Ice.** The important role sea ice plays in the climate system and polar marine ecology depends strongly on the transfer of heat, light and fluids through the ice cover [128]. Given the remoteness of the polar oceans, there is significant interest in deriving information about transport properties (hydraulic or thermal conductivity, optical properties, etc.) from remote sensing data [9, 68, 94], which in turn requires a more detailed understanding of the links between dielectric and transport properties. There

have only been very limited studies along these lines in sea ice research. For example, Barber and co-workers examined links between dielectric properties and the heat budget of Arctic sea ice and were able to show close coupling between the shortwave radiation budget and radar backscatter signatures [9, 82].

In this project, we aim to derive information about key sea-ice state variables, in particular the brine volume fraction, and morphology and connectivity of the pore space from measurements of electromagnetic properties. Earlier work [70, 112] has provided evidence for a critical transition in sea ice permeability for  $\phi$  around 0.05 to 0.07. Monitoring such transitions in the field presents considerable challenges, but preliminary results from borehole tomography suggest that this approach holds promise in tracking the movement of percolation horizons or other anomalies affecting transport of heat and fluid [84].

### 3. Mathematics of Transport in Composite Materials

There has been significant interest in low frequency and DC investigations of sea ice due their importance in measuring its thickness. In this regime the EM properties are closely related to other sea ice transport properties such as fluid permeability, and the EM response is controlled by the effective complex permittivity tensor  $\epsilon^*$ . It depends on the permittivities of the components,  $\epsilon_1$  for brine and  $\epsilon_2$  for ice, and the mixture geometry. In this frequency range the ice and brine are highly contrasting, and EM properties depend strongly on porosity, connectedness, and anisotropy of the microstructure.

**Analytic Continuation Method.** Various approximate formulas, such as the well-known Maxwell-Garnett formula, have been proposed for evaluating the effective complex permittivity of mixtures [121, 100]. Some of these formulas are semi-empirical, others are based on specific models such as dilute suspensions of spheres or ellipsoids in a host. However, inverting such formulas for inclusion volume fraction is often not accurate [147]. Moreover, we wish to recover more geometrical information than  $\phi$ . Analytic continuation provides a rigorous, robust approach to this problem.

We consider a two-phase random medium with  $\epsilon(x, \alpha)$  the local complex permittivity, a spatially stationary random field in  $x \in \mathbb{R}^d$  and  $\alpha \in \Omega$ , where  $\Omega$  is the set of realizations of the medium. Assume  $\epsilon(x) = \epsilon_1 \chi_1 + \epsilon_2 \chi_2$ , where  $\chi_j(x, \alpha)$  is the characteristic function of medium  $j = 1, 2$ , equaling 1 for  $\alpha \in \Omega$  with medium  $j$  at  $x$ , and 0 otherwise. Let  $E(x)$  and  $D(x)$  be the stationary random electric and displacement fields, related by  $D = \epsilon E$ , satisfying  $\nabla \cdot D = 0$  and  $\nabla \times E = 0$ , where  $\langle E(x) \rangle = e_k$ ,  $e_k$  is a unit vector in the  $k^{th}$  direction, for some  $k = 1, \dots, d$ , and  $\langle \cdot \rangle$  means ensemble average over  $\Omega$  or spatial average over all of  $\mathbb{R}^d$ . The effective complex permittivity tensor  $\epsilon^*$  is defined as  $\langle D \rangle = \epsilon^* \langle E \rangle$ . We focus on one diagonal coefficient  $\epsilon^* = \epsilon_{kk}^*$ , with  $\epsilon^* = \langle \epsilon E_k \rangle$ , and since  $\epsilon^*$  depends on  $h = \epsilon_1/\epsilon_2$ , we define  $m(h) = \epsilon^*/\epsilon_2$ , which is a Stieltjes function. It is analytic off  $(-\infty, 0]$  in the  $h$ -plane, and maps the upper half plane to the upper half plane [10, 61].

The key step [10, 97, 11, 98, 61, 12, 100] is obtaining an integral representation for  $\epsilon^*$ . Consider  $F(s) = 1 - m(h)$ ,  $s = 1/(1 - h)$ , which is analytic off  $[0, 1]$  in the  $s$ -plane. Then [61]

$$F(s) = 1 - \frac{\epsilon^*}{\epsilon_2} = \int_0^1 \frac{d\mu(z)}{s - z}, \quad s = \frac{1}{1 - \epsilon_1/\epsilon_2}, \quad (1)$$

where  $\mu$  is a positive measure on  $[0, 1]$ . This formula arises from the resolvent representation of the electric field  $E = (s + \Gamma \chi_1)^{-1} e_k$ , where  $\Gamma = \nabla(-\Delta)^{-1} \nabla \cdot$  and  $\Delta = \nabla^2$  is the Laplacian, yielding

$$F(s) = \langle \chi_1 [(s + \Gamma \chi_1)^{-1} e_k] \cdot e_k \rangle. \quad (2)$$

In the Hilbert space  $L^2(\Omega, P)$  with weight  $\chi_1$  in the inner product,  $\Gamma \chi_1$  is a bounded self adjoint operator. Formula (1) is the spectral representation of the resolvent, and  $\mu$  is a spectral measure of  $\Gamma \chi_1$ , in the  $e_k$  state. Formula (1) separates the component parameters in  $s$  from the geometrical information in  $\mu$ . (Extensions to multicomponent media involve several complex variables [62, 57, 101, 99, 41].) Information about the geometry enters through the moments  $\mu_n = \int_0^1 z^n d\mu(z) = (-1)^n \langle \chi_1 [(\Gamma \chi_1)^n e_k] \cdot e_k \rangle$ . Then  $\mu_0 = \phi$ , and  $\mu_1 = \phi(1 - \phi)/d$  if the material is statistically isotropic. In general,  $\mu_n$  depends on the  $(n + 1)$ -point correlation function of the medium.

Bounds on  $\epsilon^*$  are obtained by fixing  $s$  in (1), and varying over admissible measures  $\mu$ , or admissible geometries, such as those of fixed mass,  $\mu_0 = \phi$ . In this case the bounds are attained by extremal measures – Dirac point measures of the form  $\phi \delta_a(dz)$ . Higher moments of  $\mu$  can be incorporated by iterations of transformations of  $F$  [57], yielding for example, the Hashin–Shtrikman bounds [83], which assume microstructural isotropy as well as  $\phi$ . Tighter bounds [65, 69] on  $\epsilon^*$  can be obtained if the material has a matrix-particle

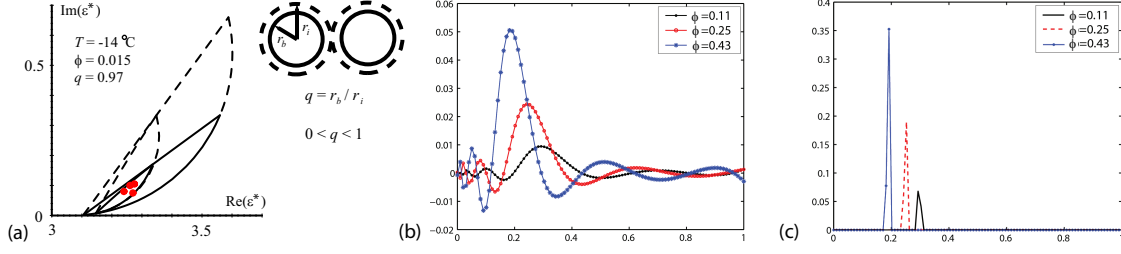


Figure 2: (a) Bounds on  $\epsilon^*$ . (b) Reconstructions of the spectral function for a Maxwell-Garnett composite using quadratic or Tikhonov regularization, and a nonnegativity constraint in (c) [33].

structure with separated inclusions. Then the support of  $\mu$  lies in  $[s_m, s_M]$ ,  $0 < s_m < s_M < 1$  [22]. The more separation, the smaller the interval, and the tighter the bounds. Comparison of 4.75 GHz data (red) on  $\epsilon^*$  for sea ice with a series of bounds [65] is shown in Figure 2 (a). The outer dotted curves are complex arithmetic and harmonic mean bounds, and the inner dotted curves are complex Hashin-Shtrikman bounds. The tighter solid bounds are matrix-particle versions. The parameter  $q$  measures the inclusion separation, and can be bounded using permittivity data [103]. Complex bounds for 50 MHz and GHz-range data [2] are in [75, 60, 65, 69]. We have inverted  $\epsilon^*$  data to obtain bounds on  $\phi$  [32, 68, 75], but now present a more powerful method for recovering microstructure.

**Reconstructing the Spectral Measure.** It has been shown in [27] that the spectral measure  $\mu$ , which contains all geometrical information about a composite, can be uniquely reconstructed if measurements of the effective permittivity  $\epsilon^*$  are available on an arc in the complex  $s$ -plane. If the component parameters depend on frequency  $\omega$ , variation of  $\omega$  in an interval  $(\omega_1, \omega_2)$  gives the required data. Reconstructing  $\mu$  can be reduced to an inverse potential problem. Indeed,  $F(s)$  admits a representation through a logarithmic potential  $\Phi$  of the measure  $\mu$  [27, 63, 64],

$$F(s) = \frac{\partial \Phi}{\partial s}, \quad \Phi(s) = \int_0^1 \ln |s - z| d\mu(z), \quad \partial/\partial s = (\partial/\partial x - i \partial/\partial y) \quad (3)$$

The potential  $\Phi$  solves the Poisson equation  $-\Delta \Phi = \rho$ , where  $\rho(z)$  is a density on  $[0, 1]$ . A solution to the forward problem is given by the Newtonian potential with  $\mu(dz) = \rho(z)dz$ . The inverse problem is to find  $\rho(z)$  (or  $\mu$ ) given values of  $\Phi, \partial \Phi / \partial n$ , or  $\nabla \Phi$ . The inverse problem is extremely ill-posed and requires regularization to develop a stable numerical algorithm.

**Regularization.** When frequency  $\omega$  varies across the interval  $(\omega_1, \omega_2)$ , the complex parameter  $s$  traces an arc  $\mathcal{C}$  in the  $s$ -plane [27]. Let  $A$  be an operator in (3) mapping the set of measures  $\mathcal{M}[0, 1]$  on the unit interval onto the set of derivatives of complex potentials defined on a curve  $\mathcal{C}$ . To construct the solution we consider the problem of minimizing  $\|A\mu - F\|^2$  over  $\mu \in \mathcal{M}$ , where  $\|\cdot\|$  is the  $L^2(\mathcal{C})$ -norm,  $F(s)$  is the measured data, and  $s \in \mathcal{C}$ . The solution does not depend continuously on the data, and regularization based on constrained minimization is needed [27, 28]. Instead of minimizing  $\|A\mu - F\|^2$  over all functions in  $\mathcal{M}$ , it is performed over a convex subset satisfying  $J(\mu) \leq \beta$ , for a stabilizing functional  $J(\mu)$  and some  $\beta > 0$ . The advantage of using quadratic  $J(\mu) = \|L\mu\|^2$ , is the linearity of the corresponding Euler equation resulting in efficiency of the numerical schemes. However, the reconstructed solution necessarily possesses a certain smoothness. Nonquadratic stabilization imposes constraints on the variation of the solution. The total variation penalization, as well as a non-negativity constraint [28], does not imply smoothness, permitting more general recovery, including the important Dirac measures.

For a Maxwell-Garnett model of a mixture of sand grains and water, with water volume fractions  $\phi = 0.11, 0.25, 0.43$ , the corresponding spectral measures are the delta functions:  $0.11 \delta_{0.297}(dz)$ ,  $0.25 \delta_{0.25}(dz)$ , and  $0.43 \delta_{0.19}(dz)$ . Simulated multi-frequency values of  $\epsilon^*$  were used in [33] to recover  $\mu$ . Reconstructions using Tikhonov (quadratic) and non-negatively constrained regularization, are in Fig. 2. While Tikhonov reconstruction gives oversmoothed curves, the others are almost exact, with moments from both approaches agreeing closely. Another approach to reconstructing  $\mu$  [147, 146, 29] is based on constrained Padé approximation of  $F(s)$ , where  $\mu$  is obtained via constrained, least squares minimization.



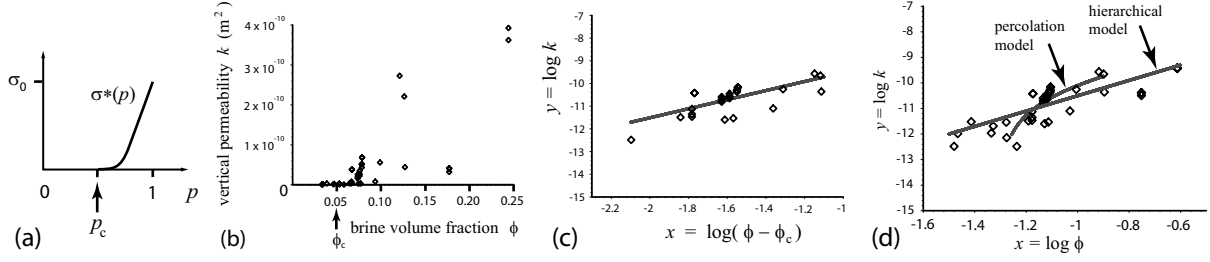


Figure 3: (a) The effective conductivity  $\sigma^*(p)$  in a percolation model. (b) Data for  $k$  taken *in situ* on Arctic sea ice. (c) Comparison of data on  $k$  in the critical regime near  $\phi_c$  with percolation theory [70]. In logarithmic variables the predicted line has the equation  $y = 2x - 7.5$ , while a best fit yields  $y = 2.07x - 7.45$ . (d) Comparison of all our data with the hierarchical model [70]. The predicted line has the equation  $y = 3x - 7.5$ , while a best fit yields  $y = 3.05x - 7.50$ .

**Percolation and Hierarchical Models.** Consider the  $d$ -dimensional integer lattice  $\mathbb{Z}^d$ , and the square or cubic network of bonds joining nearest neighbor lattice sites. In the percolation model [21, 126, 74, 23], we assign to each bond a conductivity  $\sigma_0 > 0$  with probability  $p$ , meaning it is open, and with probability  $1 - p$  we assign a 0, meaning it is closed. Groups of connected open bonds are called open clusters. In this model there is a critical probability  $p_c$ ,  $0 < p_c < 1$ , called the percolation threshold, at which the average cluster size diverges and an infinite cluster appears. Let  $x, y \in \mathbb{Z}^d$  and  $\tau(x, y)$  be the probability that  $x$  and  $y$  belong to the same open cluster. Then for  $p < p_c$ ,  $\tau(x, y) \sim e^{-|x-y|/\xi(p)}$ , and the correlation length  $\xi(p) \sim (p - p_c)^{-\nu}$  diverges with a universal critical exponent  $\nu$  (depending only on dimension) as  $p \rightarrow p_c^-$  (Fig. 1 (d)).

The effective conductivity  $\sigma^*(p)$ , defined via Kirchoff's laws, vanishes for  $p < p_c$ . Near  $p_c$  with  $p > p_c$ ,  $\sigma^*(p) > 0$  is believed to exhibit power law behavior  $\sigma^*(p) \sim \sigma_0(p - p_c)^t$ ,  $p \rightarrow p_c^+$ , where  $t$  is the conductivity critical exponent, with  $1 \leq t \leq 2$  in  $d = 2, 3$  [58, 59, 66], and numerical values  $t \approx 1.3$  in  $d = 2$  and  $t \approx 2.0$  in  $d = 3$  [126]. Consider a random pipe network with fluid permeability  $\kappa^*(p)$  exhibiting similar behavior  $\kappa^*(p) \sim \kappa_0(p - p_c)^e$ , where  $e$  is the permeability critical exponent, with  $e = t$  [24, 118, 66]. Both  $t$  and  $e$  are believed to be universal – they depend only on dimension and not the lattice. Continuum models can exhibit nonuniversal behavior with exponents different from the lattice case and  $e \neq t$  [81, 47, 126, 117, 87].

Data on the vertical fluid permeability  $k$  of sea ice, shown in Figure 3 (b), is compared with percolation theory [70] in (c), with  $k(\phi) \sim k_0(\phi - \phi_c)^2$ . The exponent  $e$  takes the universal lattice value  $t \approx 2.0$  from the general structure of the brine inclusion distribution function [106], and the scaling factor  $k_0 \approx 3 \times 10^{-8} \text{ m}^2$  is estimated using critical path analysis [50, 73]. In (d) all the data is compared with  $k(\phi) = k_0\phi^3$  for a hierarchical model of brine coated spheres of all sizes [70].

## 4. Proposed Research

We propose a range of coordinated mathematical, computational, laboratory, and field investigations. They will address the **forward problem** – how sea ice microstructure determines its low-frequency electromagnetic behavior, and in turn, the **inverse problem** – how to image the permittivity structure of sea ice and invert the data to reconstruct its internal state and transport processes. To monitor other transport properties from EM data, we will develop **cross-property relations** and novel representations for fluid and thermal transport properties.

### 4.1 Forward EM Modeling and Measurements

- **Microstructural analysis.** We plan to characterize the crystal and pore microstructure, which has substantial impact on EM properties, e.g., [137, 69, 109]. For microstructural analysis we will employ both destructive (thin-section analysis for ice crystal morphology [43]) and non-destructive techniques (X-ray tomography [70]). Building on our previous work we will investigate pore connectivity and anisotropy. Brine networks with pore and throat data will be analyzed through a percolation theoretic lens, yielding efficient computations of the spectral measure, correlation functions, and transport properties. We will identify such quantities as correlation lengths, critical paths [73, 70], and cluster sizes. Such analyses will allow for quantitative comparisons between granular and columnar ice.



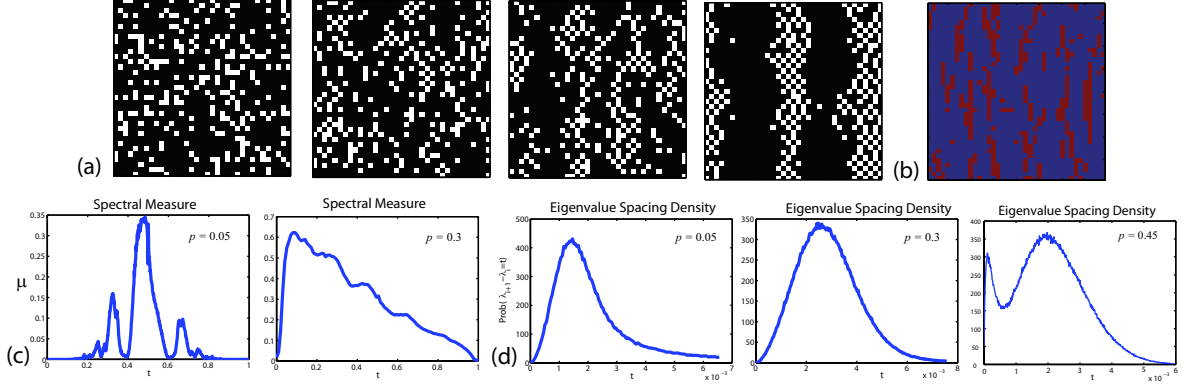


Figure 4: (a) A simulated annealing model of microstructural evolution in electrorheological fluids. Long range order develops as the applied electric field is increased and exceeds a critical value (left to right) – similar to sea ice as temperature increases. The system tends to the ground state determined by the Gibbs factor associated with a system Hamiltonian. (b) Noise is introduced in the evolution, and chain structures formed by the particles resemble connected brine structures in sea ice. (c) Evolution of the spectral measures  $\mu$  and (d) eigenvalue spacing densities as  $p$  increases for a 2D checkerboard. We anticipate qualitatively similar behavior in sea ice microstructure as temperature increases.

• **Analytical and Numerical Modeling of the Complex Permittivity.** We will bring to bear the full suite of theoretical models for composite materials to low-frequency EM behavior of sea ice. In initial investigations, we will use our microstructural analyses to obtain rigorous bounds on  $\epsilon^*$  via analytic continuation and compare with data from the direct measurements described below. Such results will provide benchmarks to judge subsequent analytical and numerical models and calculations. We will also investigate various mixing and approximate formulas and their applicability to sea ice, paying particular attention to the transitional behavior of the complex permittivity and DC conductivity with percolation and hierarchical models. However, classic percolation approaches assume infinite contrast in the component parameters. At 50 MHz,  $\epsilon_1 = 63.3 + i1930$  in brine and  $\epsilon_2 = 3.06$  in ice, which is high contrast, but not infinite. While there are approximate formulas for dealing with this situation, we will focus primarily on developing a new, more powerful approach of directly calculating the spectral measure  $\mu$  in equation (1) from our tomographic data. Such an approach will also allow us to compute thermal and DC electrical properties, and help in developing new spectral representations for fluid transport.

While there has been progress [37, 38, 127] in the past on obtaining  $\mu$ , such as the seminal results in [37] for the two dimensional random resistor network with conductivities  $\sigma_1$  and  $\sigma_2$  in the volume fractions  $p$  and  $1-p$ , respectively, the approach there focused on first computing the effective conductivity  $\sigma^*$ . Then the density  $\rho(z)$  of  $\mu$ , with  $\mu(dz) = \rho(z)dz$ , is extracted via the limit  $\rho(z) = \frac{1}{\pi} \lim_{\delta \rightarrow 0} \text{Im}[m(z + i\delta)]$  for  $z \in [0, 1]$ , and  $m = \sigma^*/\sigma_2 = 1 - F$ . Here we propose to construct the spectral measure  $\mu$  directly by finding the eigenvalues  $\lambda_i$  and eigenvectors  $\psi_i$  of matrix discretizations of the operator  $\Gamma\chi_1$  in (2), which can then be viewed as a random matrix. The indicator function  $\chi_1$  is determined by our tomographic data on the brine microstructure. With  $\psi_i\psi_i^T$  the projection onto the eigenspace of  $\lambda_i$ ,

$$\mu(d\lambda) = \sum_{i=1}^N \mu_i \delta_{\lambda_i}(d\lambda), \quad \mu_i = \langle e_k \cdot \psi_i \psi_i^T e_k \rangle, \quad (4)$$

where  $\langle f \cdot g \rangle$  here denotes an appropriate inner product. As an initial example of this approach, we have constructed the spectral measure for the discretization where  $\Gamma$  operates on periodic functions on an  $n \times n$  square, which are represented with Fourier series. The Fourier series is truncated so that the number of components equals the number of pixels  $n^2$  in the square. Then the composition with  $\chi_1$  is easily implemented. We then take the underlying medium to correspond to a two dimensional random checkerboard with component volume fractions  $p$  and  $1-p$ . The inner product in (4) is then in  $\mathbb{R}^N$ , where  $N = 2n^2$ , with an average over realizations, and  $e_k$  is a vector in  $\mathbb{R}^N$  corresponding to a standard unit basis vector for the checkerboard. Spectral measures for two values of  $p$  are shown in Figure 4 (c). We plan to develop efficient methods for computing the spectral measure from our tomographic data. For example, we

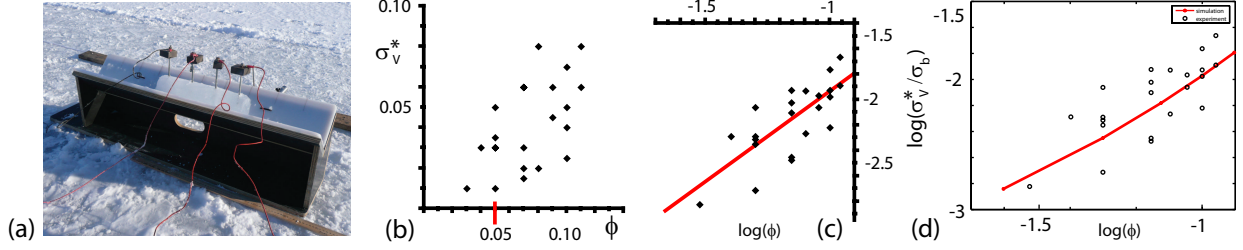


Figure 5: (a) Measurements by Golden and Gully of the vertical conductivity  $\sigma_v^*$  in Antarctic sea ice cores [71]. (b) The conductivity data is consistent with a percolation threshold. (c) The slope of the line best fitting log-log data on the form factor is  $m = 1.42$ . (d) Comparison of the form factor data with a new adaptation of our random pipe network model [148, 70] to DC conductivity.

will investigate multiscale techniques, where the underlying partial differential equation for  $\Gamma_{\chi_1}$  is solved for model pore configurations, and small-scale information is *up-scaled* and incorporated into more efficient, larger-scale discretizations. We will also investigate construction of  $\mu$  by finding the correlation functions of the microstructure from the tomographic data, which yield its moments, and then use techniques in [33].

By investigating spectral measures for sea ice microstructure and their evolution with temperature, not only do we lay the foundation for inversions using borehole arrays described below, but open up the analysis of sea ice microstructure and transport properties to sophisticated methods in statistical physics [129, 8, 63, 64] and the theory of random matrices [96, 105, 88, 40]. For example, we observe a gap in the spectrum in Figure 4 (c) for  $p = 0.05$ . In percolation theory this gap vanishes as  $p \rightarrow p_c$  with a critical exponent  $\Delta$ , and this exponent is related to critical exponents for transport via the classical scaling relations of statistical mechanics [64]. By constructing  $\mu$  directly from the spectrum, we obtain information about the eigenvalue spacing distribution (and its evolution with temperature), which is a main focus in the beautiful theory of random matrices. In Figure 4 (d) we see a transition in the type of spacing distribution as  $p$  changes, which is characteristic of transitions from disorder to order. While the  $p = 0.05$  and  $p = 0.3$  cases exhibit Poisson-like and Wigner distributions similar to those seen in mesoscopic disordered conductors and many other systems [102], the case  $p = 0.45$  near the percolation threshold appears to exhibit a new type of behavior, characterized by an accumulation of closely spaced eigenvalues. Investigating such transitions in sea ice will yield interesting insights into its transport behavior and microstructural evolution. In random matrix theory the equilibrium spectral measure minimizes a logarithmic free energy similar to the Ising model [8], and composite materials [63, 64]. This suggests a similar characterization of the thermal evolution of the brine phase in sea ice, which we plan to investigate. This type of evolution is shown in Figure 4 (a) and (b).

• **Network modeling.** In previous work [148, 70] we developed a random pipe network model to estimate the fluid permeability of a porous medium. The pipe radii are chosen from lognormal distributions describing the brine inclusions [106]. We calculated not only the effective behavior, but the local potential. With the lognormal distribution, the resulting linear system can become ill-conditioned. We developed a fast multigrid algorithm especially targeted at this unusual linear system. Tests demonstrate that this algorithm is robust, accurate, and efficient.

Here we propose to extend the multigrid numerical model we used for fluid transport to conductivity and especially complex permittivity. In seeking efficient iterative approaches to reduce various Fourier modes in the error of a solution, our method will use different network refinement levels to their advantage to solve the resulting large linear system that incorporates network features. This model will help predict the EM response of sea ice based on microstructural information, and aid in cross-property investigations. Longer range goals include development of a fast mutigrid model to calculate transport in the random brine network graphs which are output from X-ray CT, and to incorporate fluid network models into new models of thermal transport with advective contributions.

• **Direct measurements on cores.** During the SIPEX expedition in 2007, Golden and Gully adapted an earth resistance tester to measure the vertical conductivity  $\sigma_v^*$  of sea ice over 0.1 m segments, as shown in Figure 5 (a). At the same locations, we conducted Wenner soundings, measured the vertical fluid permeability  $k$ , and Kazu Tateyama measured thickness with an EM induction device. In Figure 5 (c),

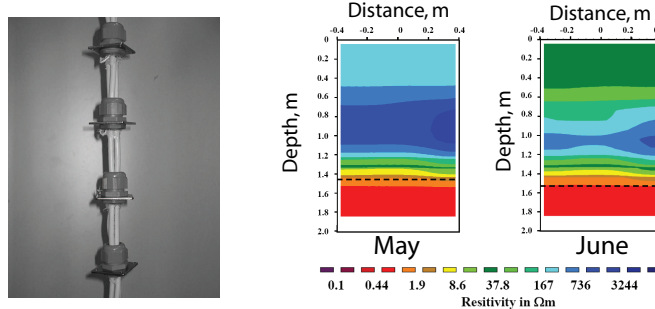


Figure 6: Cross-borehole electrode array with reconstructed resistivity images on the right [84].

formation factor data  $\mathcal{F} = \sigma^*/\sigma_1$ , is shown, where  $\sigma_1$  is the brine conductivity, which depends on  $T$  (or  $\phi$ ). Preliminary results show that the hierarchical model used to predict permeability [70] yields  $\sigma_V^*/\sigma_1 = \phi^m$  with  $m = 3/2$ , close to the best fit of 1.42.

We propose extensive measurements of electrical conductivity and permittivity from DC to 110 MHz on extracted ice cores. Based on earlier work, brine loss will be minimized by sealing the core with neoprene sleeves prior to sampling [35]. A special holder to couple the measurement tools to the ice samples will be built and tested by a senior in electrical engineering under the direction of Dr. Cynthia Furse for his/her senior capstone design project. The measurement system will be tested in the lab at UAF for ice samples at controlled temperatures, and will then be field tested in Barrow, AK. During the austral spring 2011 aboard the Aurora we will measure conductivity, permittivity and fluid permability. In McMurdo, time series measurements will be taken in a localized area during the spring transition periods in 2010 and 2012. Core samples will also be taken for structural analysis to distinguish between columnar and granular samples. Given the lack of data between 1 MHz and 100 MHz and its increasing importance for in situ measurements, low frequency remote sensing, and radar sounding [7, 115], we will focus on this frequency range.

## 4.2. Inverse EM Measurements and Reconstructions

*Geoelectrics and EM Induction Instruments.* Early DC resistivity measurements on sea ice were aimed at determining ice thickness [51, 130, 131]. Initially all these studies employed surface soundings using 4 electrodes in either the Wenner or Schlumberger configurations. The anisotropic nature of sea ice resistivity, due to brine vertical alignment and connectivity, leads to such measurements significantly underestimating the ice thickness by a factor  $\sqrt{\rho_V^*/\rho_H^*}$  where  $\rho_V^*$  and  $\rho_H^*$  are, respectively, the vertical and horizontal components of the bulk resistivity [14]. Surface measurements also lead only to an estimate of the geometric mean resistivity  $\sqrt{\rho_V^*\rho_H^*}$ .

More promising determinations of thickness have been achieved using low frequency EM techniques [79, 76, 78, 144, 116], which rely on a time varying primary magnetic field (generated by a transmitter coil) inducing eddy currents in the seawater beneath the comparatively resistive ice. The secondary magnetic field produced is sensed by a receiver coil, determining an apparent conductivity resulting from an integration between the instrument and induced currents. The thickness is found using empirical relationships [77], and the technique is adaptable for use from a helicopter or ship [76].

- **Cross-Borehole Tomography.** Cross-borehole resistivity tomography, generally used in shallow engineering and hydrological studies [36, 39, 136], has recently been demonstrated by Ingham et al. [84] to have the potential to circumvent the problems related to anisotropy that make resistivity soundings difficult to interpret in terms of ice microstructure. In particular, development of the theory of measurements in an anisotropic medium [14] shows that using only two boreholes, it is possible to make measurements that are sensitive only to  $\rho_H^*$ .

The cross-borehole technique [84] uses vertical strings of electrodes, spaced at 0.1 m intervals, frozen into ice. Passing current and measuring potential differences between electrodes in different boreholes spaced  $\approx 1$  m apart, ensures that undisturbed ice is sampled, and allows for a tomographic image of  $\rho_H^*$  via 2D or 3D inversion, as shown in Figure 6. As the lowermost electrodes are in seawater, the ice/water interface (dotted line) is also imaged. Measurements made over April-June 2006 showed a significant

decrease in  $\rho_H$  as the ice warmed, likely related to a percolation transition.

Further development of the theory of cross-borehole soundings in an anisotropic medium shows that using electrodes from at or near the same vertical level in a minimum of 4 vertical strings of electrodes allows tomographic images of the geometric mean resistivity  $\sqrt{\rho_V^* \rho_H^*}$  to be obtained. Measurements made on landfast first year ice at Barrow, Alaska in April-June 2008 using 4 boreholes arranged at the corners of a 1 m square, have not only successfully demonstrated this [86], but using the 6 separate combinations of borehole pairs also provided increased resolution of  $\rho_H^*$  in the ice volume. Inversion models for both  $\rho_H^*$  and  $\sqrt{\rho_V^* \rho_H^*}$  have then be used to derive  $\rho_V^*$ , thus solving for the anisotropy.

We will employ *in situ* borehole and surface geoelectric array measurements that have been used successfully in the past by our team to invert tomographic data sets [84]. A major innovation we propose here will be to develop a borehole array for measuring complex permittivity (led by our New Zealand partners) and to link such measurements directly to microstructural and core sample data. From data representing the amplitude ratio of the measured potential difference and current obtained from AC measurements, we will derive models of the magnitude of the complex conductivity  $\sigma^*$  (with real and imaginary parts  $\sigma'$  and  $\sigma''$ ). This magnitude is related to the complex permittivity via  $|\sigma^*| = \sqrt{\sigma'^2 + \sigma''^2} = \omega\epsilon_0\sqrt{\epsilon'^2 + \epsilon''^2}$ . Previous measurements [1] suggest that  $\epsilon'' = \sigma' / (\omega\epsilon_0)$ , where  $\sigma'$  is the DC conductivity from cross-borehole DC tomography. The combination of AC and DC measurements will then be used to derive  $\epsilon'$  giving the complete complex permittivity without addressing the issue of phase measurement in AC tomography. Through numerical simulations and lab experiments, we will ensure the electrodes are designed to minimize the effect of electrode-related impedance. Electrode strings will be frozen into first year ice as early in the season as possible and repeat measurements made over the period of spring warming. Measurements of the thermal profile using embedded thermistor strings will aid in our studies of physical properties and microstructure.

- **Spectral measure reconstruction.** We will develop methods of regularized recovery of spectral measures, and hence the microstructural state, from sea ice permittivity measurements. Additional microgeometrical information obtained from X-ray CT data on cores, as well as resistivity data, will help constrain the problem, and be incorporated into the regularized algorithms. We will develop recovery techniques based on (partial) knowledge of microstructural correlation functions, or spectral moments, obtained from X-ray CT. For instance, knowledge of  $\mu_0$  (or  $\phi$ ) results in a linear programming algorithm; if all moments are known, this approach is related to the classical Hausdorff moment problem. The proposed method will use a partial number of moments to stabilize the inversion and will likely have other applications.

Regularized Padé approximation methods will be developed to allow for accurate approximation of the support of the measure and recovery of the microstructural *partition function* [63, 64]. The distance from the support of  $\mu$  to the origin will give an estimate for the thermal distance to percolation. The zeros of the partition function will be found from zeros of the denominators of Padé approximants [29].

Since  $F(s)$  is a Cauchy transform of the spectral measure, we propose to recover not only  $\mu$ , but the operator itself. Indeed, the Padé approximation to the spectral representation can be used to construct the set of polynomials orthogonal with respect to  $\mu$ ; this set will be used to find the Jacobi matrix and the corresponding finite-difference operator. Constructed in this way, the operator can be viewed as a network approximation, which will allow us to relate a set of graphs that describe the CT-imaged brine microstructure to the set of equivalent transport networks.

### 4.3. Cross-Property Relations

Different effective properties of a composite are coupled through its microgeometry. The problem of formalizing this coupling is important for indirect evaluation of the fluid permeability and thermal conductivity of sea ice when direct measurements are difficult to make. Implicit accounting of the composite geometry was exploited in pioneering work [108] in deriving coupled bounds on material properties. Coupled or cross-property bounds use measurements of one property to improve bounds on other ones. The work of Prager was followed by many others (see references in monographs [25, 100, 132]). Empirical relations or those derived for specific geometries are used in practice, such as the Kozeny-Carman or Katz-Thompson relations [6, 13, 132]. In some models, electrical and fluid transport properties can be computed [70, 119, 143].

- **Spectral coupling.** A particularly powerful application of the inverse homogenization [27] approach we propose to take here, is that once the spectral measure has been reconstructed by inverting complex permittivity data over frequency, it can be used to calculate other effective properties such as DC electrical

conductivity and thermal conductivity. These other transport properties have identical integral representations, but involving the ratio of the relevant component parameters. Thus, through this spectral coupling, other transport properties can be estimated indirectly from EM monitoring [28, 34].

- **Permeability measurements.** Electrical studies will be complemented by permeability measurements on selected samples to help understand linkages between fluid and charge transport. Samples will be extracted in the field and the brine removed using centrifugation [142, 49]. A permeameter [48] will be used in the lab at UAF. In the Antarctic we will measure permeability by taking partial cores and timing brine inflow, wherever we do electrical measurements. We'll also be testing the use of "packers" to block out horizontal influx.

- **Connecting representations for electrical, fluid, and thermal transport.** Once we have constructed a spectral measure from permittivity measurements or through direct computations from brine tomography, we can use it to compute the DC resistivity or thermal conductivity. We will also investigate the use of other rigorous connections between electrical and fluid transport in porous media, such as in [6], and those that can be computed for particular microstructural models.

While fluid permeability differs from electrical conductivity due to a length scale in the fluid problem not present for electricity, we have recently observed an interesting rigorous connection. In obtaining our lognormal pipe bound [70, 72, 133], the analysis focused on a trapping constant  $\gamma$  for a diffusion process in the pore space. This parameter is rigorously related to permeability, with  $\mathbf{k} \leq \gamma^{-1}\mathbf{I}$ , where  $\mathbf{k}$  is the fluid permeability tensor [132, 133]. Here we propose to develop an analytic continuation and spectral measure approach to studying the trapping constant through a resolvent representation formula analogous to  $E = (s + \Gamma\chi_1)^{-1}e_k$ , which involves the same operator  $\Gamma\chi_1$ . Such an advance would open up a non-variational approach to bounding and analyzing fluid permeability properties, and would have applications to enzymatic bacterial foraging and other processes [138, 72] in sea ice and fluid-filled porous media.

Consider the problem of a tracer diffusing in the fluid (brine) phase  $V_b$  of a porous medium occupying  $V \subset \mathbb{R}^3$ . The tracer reacts with partially or completely absorbing *traps* on the boundary  $\partial V_b$  of the pore space. Let  $c(x, t)$  with  $x \in V_b$  be the time dependent concentration of the reactant governed by the diffusion equation and boundary condition

$$\frac{\partial c}{\partial t} = D_1 \Delta c + G, \quad x \in V_b, \quad D_1 \frac{\partial c}{\partial n} + \eta c = 0, \quad x \in \partial V_b, \quad (5)$$

where  $D_1$  is the diffusion coefficient of the reactant in the fluid,  $\eta$  is a positive surface reaction rate constant,  $G$  is a generation rate of reactant per unit trap-free volume, and  $n$  is the unit outward normal from the pore space. In the diffusion-controlled limit [133], where a reactant will typically diffuse in the pore space for much longer than the characteristic time associated with the surface reaction, we consider the steady state problem where the rate of removal of the reactant by absorbing boundaries is exactly compensated by the production rate per unit volume  $G$  of the reactant. The parameter of interest is the *trapping constant*,

$$\gamma^{-1} = \langle u\chi_1 \rangle, \quad \Delta u = -1, \quad x \in V_b, \quad u = 0, \quad x \in \partial V_b, \quad (6)$$

where  $u$  is a scaled concentration field obtained from a two-scale expansion of  $c$ . The trapping constant is inversely related to the *mean survival time*  $\tau$  for diffusion in the pore space,  $\tau = 1/\gamma\phi D_1$ . We now allow the tracer to diffuse into the solid (ice) phase by assigning it the diffusion coefficient  $D_2 > 0$  (where we will be eventually interested in the limiting behavior as  $D_2 \rightarrow 0$ ), and consider the following generalization  $\nabla \cdot ((D_1\chi_1 + D_2\chi_2)\nabla u) = -\chi_1$  of  $\Delta u = -1$ . With  $h = D_2/D_1$  and  $s = 1/(1 - h)$ , this equation yields a resolvent representation for  $J = -D_1\nabla u$ ,

$$J = s(s + \Gamma\chi_1)^{-1}f, \quad f = \nabla(-\Delta)^{-1}\chi_1. \quad (7)$$

We plan to develop a spectral representation for  $\gamma$  based on (7), involving the spectral measure obtained through brine tomography or inversion, and use it study fluid transport and diffusion in the brine pore space.

Finally, electrical monitoring can tell us about fluid transport, which in turn can give data on advective contributions to thermal transport [95, 134]. Avellaneda and Majda [4, 5] obtained a Stieltjes integral representation via analytic continuation in the Peclet number, quite similar to (1), of the effective diffusivity for transport of a scalar  $T$  (here temperature or salinity) by a steady incompressible velocity field  $v$ ,

$$\frac{\partial T}{\partial t} + v \cdot \nabla T = D\Delta T, \quad \nabla \cdot v = 0, \quad \langle v \rangle = 0. \quad (8)$$

Now the spectral measure depends on flow geometry. We plan to exploit this framework, along with information about fluid flow in sea ice and our permeability results, to investigate thermal diffusivity in sea ice when brine advection contributes to thermal transport, as well as salinity profile evolution.

**Impact of the Proposed Work:** Brine inclusions are critical in determining the state of the sea ice, its properties and the transfer of energy and matter through it. The proposed work is a timely contribution aimed at developing methods that allow the *in situ*, non-destructive measurement of specific transport variables, as well as the interpretation and inversion of this data in a theoretical framework. The latter should significantly improve our ability to monitor critical aspects of the ice cover (such as flooding by seawater, drainage of surface ponds, increases in porosity leading to substantial reductions in ice strength, etc.) in the context of its important role in the polar environment and in predicting climate change. The mathematical components of this work, such as the derivation of spectral measures for specific ice types will be the first step in linking standard measures of ice microstructure (such as pore size or number density) to measures (such as the n-point correlation function) that can link different properties or processes to the more fundamental aspects of ice microstructural evolution. This is not only of academic interest, but can also help inform the design and implementation of emerging polar observing networks that will rely increasingly on indirect measurements via drifting sensors or remote sensing. Because of the broad range of properties and techniques covered, our work will contribute to understanding transport in porous media in general.

### **Experimental Timeline**

**Year 1 (1 Oct. 2009 – 30 Sept. 2010).** Assemble and test set-up for electrical measurements on ice cores; build borehole arrays and deploy in Barrow, AK, in February 2010. Retrieve borehole arrays in Barrow and begin electrical measurements on cores and permeability studies, May 2010.

**Year 2 (1 Oct. 2010 – 30 Sept. 2011).** Make direct electrical and permeability measurements in Antarctica (McMurdo/Scott) in Dec. 2010. Complete first set of ice core measurements and microstructural analysis in spring 2011. Continue borehole and direct measurements in Barrow, freeze-in February 2011, retrieval and spring measurements in May 2011. Prepare borehole arrays for Antarctic deployment in McMurdo/Scott.

**Year 3. (1 Oct. 2011 – 30 Sept. 2012).** Improve/refine design of electrical measurements on cores and permeability studies, for use in Oct.-Nov. 2011 aboard the *Aurora Australis*, via ice station sampling at many locations. Complete analysis of Barrow samples. Freeze-in deployment of borehole array in McMurdo/Scott, Antarctica, austral spring 2012. Continue borehole and direct measurements in Barrow, freeze-in Feb. 2012, retrieval and spring measurements in May 2012.

**Year 4. (1 Oct. 2012 – 30 Sept. 2013).** Retrieve Antarctic borehole arrays, final direct measurements on cores and permeability, Dec. 2012. Complete core measurements; complete data analysis and synthesis of transport property measurements.

**Management Plan:** The UU team (led by Golden) will be responsible for forward and inverse modeling of the EM properties of sea ice, and for developing a device to measure the complex permittivity of sea ice cores. Golden and Furse will conduct Arctic and Antarctic field measurements with students and the post-doc. The UAF team (led by Eicken) will be responsible for pore and crystal microstructure studies necessary to interpret electrical measurements. In addition, the team will measure permeability on selected samples. The UAF team will coordinate and organize the field measurements at Barrow, AK with later lab analysis in the UAF Geophysical Institute Cold Lab. Finally, the UAF group will lead the analysis of microstructural and permeability data in conjunction with electric data. The VUW team (led by Ingham) will be responsible for developing the cross-borehole arrays and for deployment in the Arctic and Antarctic, and to extend their use from DC to AC. Overall responsibility for success of the project, and integration of the theoretical and experimental components, rests with the PI Golden.

**Modes of Collaboration and Training:** Throughout the project we will build on successful approaches from our past and ongoing collaboration to assemble diverse field teams, comprising undergraduate and graduate students, senior researchers and post-docs with a variety of backgrounds to enhance cross-disciplinary exchange between mathematicians, geophysicists and engineers. Through the UAF group, we will also be able to discuss our work in the context of traditional Inupiaq Eskimo knowledge of sea ice, which places great importance on the observation of key transport processes, such as flooding of sea ice or melt pond formation. As a major contribution to the training of graduate and undergraduate students and post-docs, and a novel mode of exchange, we will bring a group of mathematicians, geophysicists and

other experts and students into the field for a sea-ice field course (led by Eicken) in Year 3 of the study. This course will be held in Barrow and build on the expertise at UAF in holding such interdisciplinary courses. The course will build on a textbook developed by Eicken and others, that is currently in the final stages of editing with the University of Alaska Press. We strongly believe in the value of immersion of a diverse group of people into a field research setting to stimulate scientific discovery and exchange, and we will use this opportunity in Barrow to transition into the final stages of our project.

**Postdoctoral Mentoring:** The postdoctoral fellow will be based in the Math Department at Utah with Golden, but will be involved in a broad range of highly interdisciplinary activities. These include: theoretical and computational investigations into the EM behavior of sea ice microstructure and the role of transport processes in polar climate models; aiding in the development of permittivity measurement techniques for ice cores; field work in the Arctic and Antarctic; a sea ice field-course in Barrow; regular interactions with Eicken, Ingham and colleagues in Geophysics at UAF and Physics at VUW, and with Furse in Electrical Engineering at Utah; delivering lectures at conferences; helping to mentor REU and graduate students. He or she will meet formally with Golden once a week, with many more informal interactions, and likely just as often with Cherkaev and Zhu.

**Outreach and Broader Impact:** As described in Results from Prior NSF Support and the Biographies, the investigators have been extensively involved in outreach to students and broader communities. We have been actively involved in addressing the broader impact of our work and its connection to climate change – Golden is chair of the national Committee for Math Awareness Month April 2009 on Mathematics and Climate ([www.mathaware.org](http://www.mathaware.org)), on behalf of the Joint Policy Board for Mathematics. Golden and Furse have both been very active in undergraduate education, and in attracting students into science, engineering, and math. We anticipate that this project will fuel even more success in this direction, particularly since it combines math, geophysics, engineering, questions of climate change, and the prospect of Arctic and Antarctic field work. Eicken and Golden plan to bring together mathematical and geophysical scientists at an AGU session on transport in sea ice. Furse is leading a large statewide effort in Utah to bring more students into engineering and science, and will use this project and its relation to climate change as a valuable tool in this effort, particularly for student summer engineering camps, teacher training, etc.

**Statement of Eligibility for CMG:** A broad range of processes in the polar marine environment such as snow-ice formation, the evolution of melt ponds and sea ice albedo, and biomass build-up, depend upon fluid, thermal, and electromagnetic transport in sea ice. Understanding these processes and the microstructural properties of sea ice which control them, is at the forefront of polar climate science. Current climate and biogeochemical models seeking to predict the future of Arctic and Antarctic sea ice and the response of polar ecosystems in the face of continued warming, in general do not incorporate such processes in a realistic fashion. For example, current estimates for the disappearance of summer Arctic sea ice range from several years to many decades, depending on how summer ice albedo, which depends on retention of melt-water at the ice surface, is represented in the model. Refining such predictions of the ice cover's role in the climate system requires realistic assessment, monitoring and understanding of these transport processes. Our proposed research is aimed at the heart of this highly interdisciplinary problem, requiring cutting-edge contributions from mathematics, geophysics, and electrical engineering. Our proposal relies on interlacing theoretical advances in areas of applied mathematics, such as inverse homogenization and theories of critical phenomena, with state-of-the-art EM measurement techniques to be carried out in some of the most extreme environments of the world, the Arctic and Antarctic ice packs. Success on these diverse fronts, and synthesizing the approaches to achieve important results, relies on an effective collaboration between mathematicians, geophysicists, and electrical engineers. We believe we have assembled such a team, and have the relevant background and experience to accomplish the proposed work.